


RESEARCH ARTICLE

# Fast optimization of sparse antenna array using numerical Green's function and genetic algorithm

Mordecai F. Raji | Huapeng Zhao  | Happy N. Monday

School of Electronic Science and Engineering, University of Electronic Science and Technology of China, Chengdu, China

## Correspondence

Huapeng Zhao, School of Electronic Science and Engineering, University of Electronic Science and Technology of China, Chengdu, 611731, China.  
Email: huapengzhao@uestc.edu.cn

## Funding information

National Natural Science Foundation of China, Grant/Award Number: 61701087; Sichuan Science and Technology Program, Grant/Award Number: 18GJHZ

## Abstract

A single-element antenna is unfit for application in most wireless systems and an alternative is an array of antenna. The desire to reduce weight and cost of antenna arrays gave rise to sparse arrays. The design of a sparse antenna array requires an optimization process, which is time-consuming for large arrays. In order to accelerate the optimization process, a method combining the numerical Green's function (NGF) and genetic algorithm (GA) is presented in this paper. In the proposed method, binary coding is applied to describe the status of antenna elements, and GA optimization is performed to sparsify the array subject to constraint on the peak side lobe level (PSLL). The PSLL is calculated efficiently by the NGF. Simulation results are presented to illustrate the advantage of the proposed method. It is shown that the proposed method significantly reduces the optimization time.

## KEYWORDS

Green's function, optimization, genetic algorithm, peak side lobe level, sparse array

## 1 | INTRODUCTION

Sparse array antennas offer great potential in medical applications, communications, radar, remote sensing, radio astronomy, and other areas of wireless deployment.<sup>1</sup> Its advantages include higher power efficiency, reduced weight, and reduced cost. However, it comes with challenges such as unwanted side lobe and grating lobes, which causes interference to communication and results in electromagnetic compatibility problem.<sup>2</sup> A lot of methods and algorithms have been proposed to optimize antenna arrays in diverse studies.<sup>3</sup> In Daniel, Marco, Mario, and Fulvio's study,<sup>4</sup> a procedure for fast optimization of sparse antenna arrays based on the use of benchmark equispaced array (BEA) was discussed. BEA is based on using standard well-known approach as a design reference. But, this method is limited to linear arrays. Fasenfest, Capolino, and Wilton<sup>5</sup> proposed a fast method of moments (MoM) solver for a large array of printed antennas in a layered material by using Green's function interpolation and fast Fourier method (GIFFT). In contrast to these papers, this write-up aims to develop a fast antenna array optimization algorithm that can be applied to any antenna of choice.

The Green's function is suitable for expressing radiation pattern of an antenna element. The ordinary method of designing a sparse array is time-consuming because each genetic algorithm (GA) iteration step requires computation of the antenna array radiation pattern using computation-intensive methods like MoM. For large arrays, the process is more cumbersome. In the proposed method, the Green's function is obtained by the MoM solver to achieve faster calculation of the radiation pattern of the antenna element. This method allows the radiation pattern of the antenna element to be computed just once, stored, and reused in the whole GA optimization process. Based on the element radiation pattern modeled by the Green's function, an arbitrary array can be analyzed and designed. GA is used to

optimize the array to make it sparse because GA operators involve mutation and thus rarely gets trapped in local minima.<sup>6,7</sup> It should be noted that the proposed method is flexible and it could be extended by replacing GA using other global optimization techniques like the differential evolution (DE) method.<sup>8,9</sup>

The rest of this paper is organized as follows. Section 2 describes the formulation and validation of numerical Green's function (NGF) and briefly introduces GA. Section 3 presents numerical results obtained by GA optimization of sparse antenna arrays. Section 4 concludes this work.

## 2 | THE PROPOSED METHOD

### 2.1 | Antenna array modeling using NGF

The Green's function can be used to express the impulse response of a system. Without the loss of generality, we take the electric dipole and the microstrip patch antenna as examples. The electric field in the far-field region for an electric dipole is given by<sup>10</sup>

$$E_{\theta}(\theta) = j \frac{Id\ell}{4\pi} \left( \frac{e^{-jkR}}{R} \right) \eta_o k \sin\theta, \quad (1)$$

where  $Id\ell$  is the excitation current,  $\eta_o$  is the impedance of free space, and  $k$  is the free space wave number.  $k = 2\pi/\lambda$ , where  $\lambda$  is the wavelength. Here, we can ignore  $(e^{-jkR}/R)$  for far-field expression.

To formulate the radiation pattern of a patch antenna, the current distribution on the patch needs to be determined. With respect to this, the electric field integral equation (EFIE) is used in this paper. EFIE allows the calculation of electric field generated by an electric current distribution impressed upon a surface or in a volume. The EFIE is given in mixed potential form in Markarov, Kulkarni, and Marut's study.<sup>11</sup>

$$\vec{E}^i = \vec{E} + \left[ jw\vec{A}_D(\vec{r}) + \nabla\Phi_D(\vec{r}) + jw\vec{A}_M(\vec{r}) + \nabla\Phi_M(\vec{r}) \right] \quad \vec{r} \in V, \quad (2)$$

$$\vec{E}_{\tan}^i = \left[ jw\vec{A}_M(\vec{r}) + \nabla\Phi_M(\vec{r}) + jw\vec{A}_D(\vec{r}) + \nabla\Phi_D(\vec{r}) \right]_{\tan} \quad \vec{r} \in S_M. \quad (3)$$

$\vec{E}^i$  denotes the impressed field.  $\vec{A}(\vec{r})$  and  $\Phi(\vec{r})$  are the magnetic vector potential and the electric potential for the metal and dielectric, respectively.  $\vec{E}(\vec{r})$  is the total electric field. The antenna current distribution is calculated using Equations 2 and 3, and then integration of the current gives the patch antenna radiation pattern.

For electric dipole, the radiation pattern of a single radiating element is calculated by using Equation 1. For patch antenna, Equations 2 and 3 are numerically solved by the MoM to find the currents, and the radiation pattern is then calculated by numerical integration of the currents. The numerically calculated radiation pattern represents the far field response of a single radiating element. Hence, it is named as the NGF.<sup>12</sup>

For an array of antennas whose elemental mutual coupling is negligible, the field pattern  $f(\theta, \phi)$  is expressed as a product of the NGF  $E(\theta, \phi)$  and the array factor  $AF$

$$f(\theta, \phi) = E(\theta, \phi) \times AF(\theta, \phi), \quad (4)$$

where  $AF(\theta, \phi)$  for a planar array is given by Nandi<sup>13</sup>:

$$AF(\theta, \phi) = 4 \sum_{m=1}^M \sum_{n=1}^N I_{mn} e^{j\phi_{mn}} \cos[(m-0.5)\psi_x] \times \cos[(n-0.5)\psi_y]. \quad (5)$$

$$\psi_x = kd_x (\sin\theta \cos\phi - \sin\theta_0 \cos\phi_0),$$

where  $(\theta_0, \phi_0)$  represent the angle of maximum radiation,  $m$  and  $n$  are the array size, and  $dx$  and  $dy$  are the elements spacing in the  $x$ - and  $y$ -directions, respectively.

The equations in previous studies<sup>14,15</sup> were used to determine the parameters for the patch to operate at a resonant frequency of 2.4 GHz as itemized in Table 1. The dielectric medium is FR4. The substrate dimensions are the same as those of the ground plane.

With the radiation pattern of a single radiation element, Equation 4 can be used to calculate the radiation pattern of an array. The radiation pattern of a single element is stored and reused, and the calculation of array factor in Equation 5 requires little calculation time. Hence, the array radiation pattern can be calculated efficiently. In Section 3, both the electric dipole antenna array and patch antenna array radiation pattern are calculated by using Equation 4.

## 2.2 | GA formulation

The main objective of optimization is to minimize the peak side lobe level (PSLL). The GA does so by evaluating the cost function in each generation. The cost function is given by Nourinia<sup>16</sup> as follows:

$$c = \max \left| \frac{psll|AF(\theta, \phi)|}{\max|AF(\theta, \phi)|} \right|. \quad (6)$$

From the cost function evaluation, the goal function constraints can be determined. The goal function is constrained by the set values of PSLL, gain, and the percentage of the active elements which is given by

$$f(a_{11}, \dots, a_{MN}) = (loss < 1dB, fillrate < 90\%, optPSLL < InitPSLL), \quad (7)$$

**TABLE 1** Design parameters for the patch antenna

Parameter	Value
Patch length (Pl)	2.8 cm
Patch width (Pw)	3.6 cm
Ground plane length (Gpl)	3.7 cm
Ground plane width (Gpw)	4.6 cm
Substrate height (Sh)	0.15 cm
Feed point (Fp)	Pw/2, L = 0.7 cm
Dielectric (D)	FR4 = 4.8

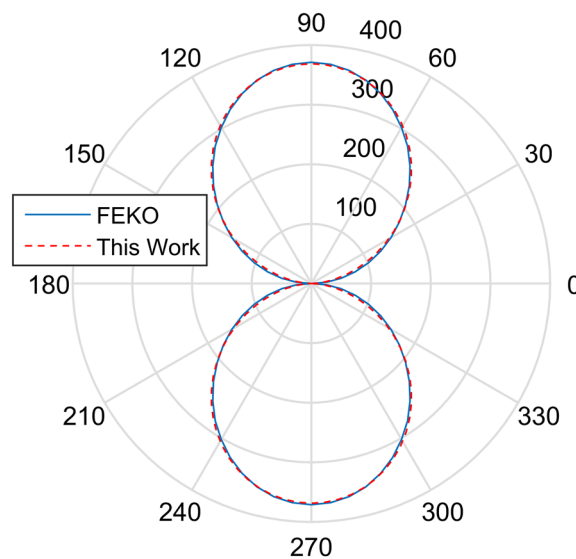


**FIGURE 1** Validation of the E-field radiation pattern of the  $1 \times 4$  linear dipole array at  $\phi = 45^\circ$ ,  $\theta = 0:360^\circ$

where  $loss$  is the gain drop and  $fillrate$  is the percentage of active elements after optimization.  $InitSLL$  and  $OptSLL$  are the PSLR before and after optimization, respectively.

Once the goal is achieved, the result is the active candidates in the population ( $a_{11}, \dots, a_{MN}$ ), which is denoted by  $\mathbf{a}$ .  $\mathbf{a}$  is a vector consisting of the excitation coefficient of all elements. Since the elements are excited in a binary state, the value of elements in  $\mathbf{a}$  can either be 1 or 0.

In the initialization stage, the selection is conditioned so that the elements toward the center are active and the dummy elements are toward the edge. At each cycle, the algorithm sorts the generation according to the cost function and discards the ones with lower performance according to the settings. It then mutates and mates the rest candidates to generate new offsprings, which will be the constituent of the next generation. The process continues until the termination criterion is met. In this case, it is set to terminate at the 100th iteration.

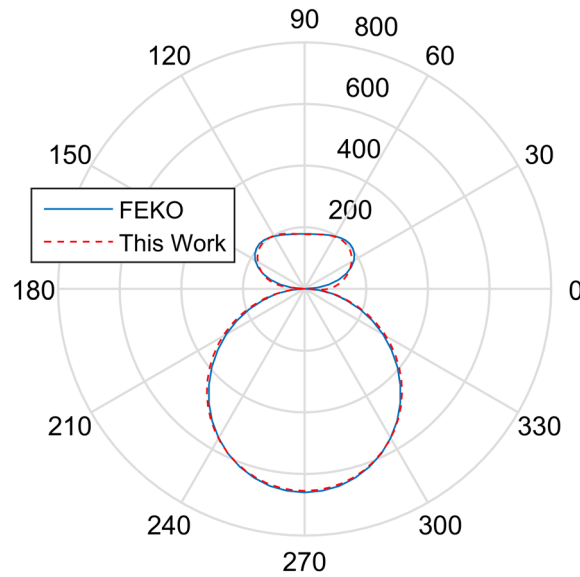


**FIGURE 2** Validation of the E-field radiation pattern of the  $3 \times 3$  planar dipole array at  $\phi = 45^\circ$ ,  $\theta = 0:360^\circ$

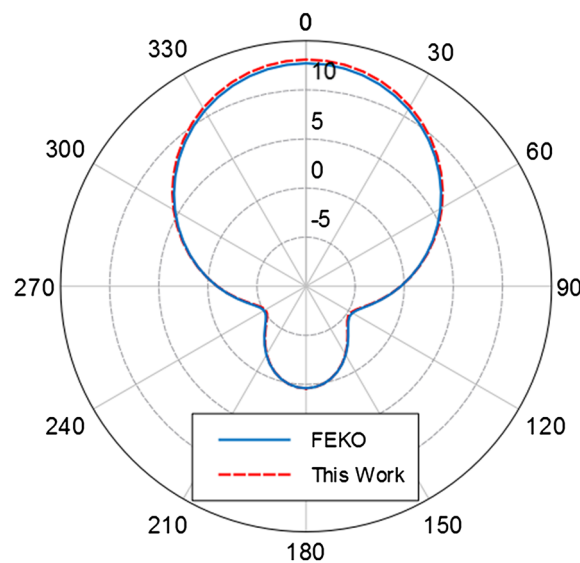


**FIGURE 3** Validation of the E-field radiation pattern of the  $2 \times 2$  patch antenna array at  $\phi = 0^\circ$ ,  $\theta = 0:360^\circ$

### 3 | NUMERICAL RESULTS

#### 3.1 | Antenna array radiation pattern validation

In this section, the theories and formulations explained in Section 2 are validated. Simulations are performed on a four-element linear array, a nine-element electric dipole planar array, and on a four-element patch antenna planar array. The planar array antennas are placed on the  $xy$ -cut planes with  $z = 0$ . The row and column interelement spacing is half wavelength. The patch antenna setup has been discussed in Section 2. Figures 1, 2, 3, and 4 show the comparison between the proposed method and the commercial software FEKO. It can be observed that the proposed method agrees well with FEKO, which indicates that the array radiation pattern can be accurately calculated by using Equation 4.

#### 3.2 | Dipole array optimization

Next, a 900-element dipole array was optimized using GA. The goal function is defined in Equation 7. Figure 5 presents the radiation pattern of the fully populated array and the optimized array. The fully populated array shows an initial PSLL of  $-13.94$  dB, and the optimized array shows PSLL of  $-16.67$  dB. Figure 6 presents the distribution of active ele-

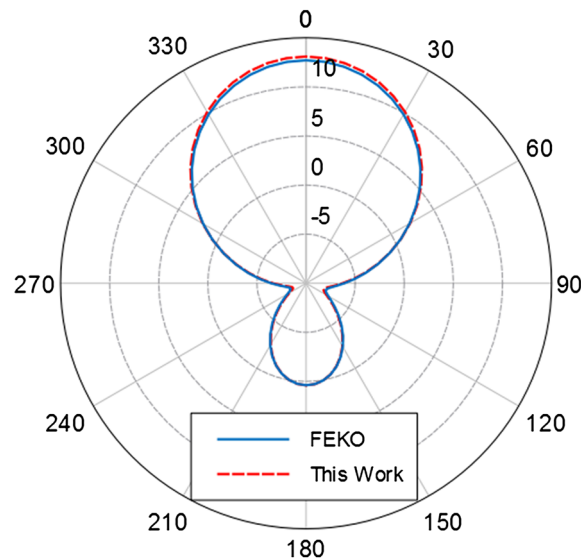


**FIGURE 4** Validation of the E-field radiation pattern of the  $2 \times 2$  patch antenna array at  $\phi = 90^\circ$ ,  $\theta = 0:360^\circ$

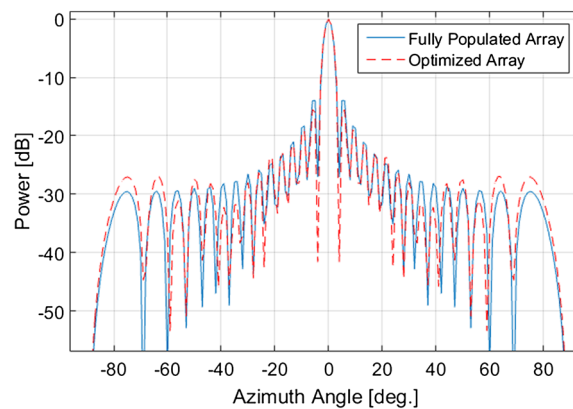


**FIGURE 5** View of the array radiation pattern at  $\theta = 0^\circ$ ,  $\phi$  varies from  $-90^\circ$  to  $90^\circ$

ments. The fillrate of the optimized array is 89%. Figure 7 shows the convergence behavior of the genetic optimization. It can be observed that the PSLL continuously drops as the number of iterations increases. Figure 5, Figure 6, and Figure 7 show that the proposed method is able to reduce the number of array elements while suppressing the PSLL.

### 3.3 | Microstrip patch antenna array optimization

Furthermore, a 400-element patch antenna array is optimized on a dual core 2.2 GHz processor. The geometry of a typical patch antenna makes it complex to generate the far-field radiation pattern compared with a dipole. The optimization of such array size (of patch antennas) using the ordinary technique (direct optimization using GA) takes a considerable amount of processing time. The method employed in this paper enables faster optimization. Figure 8 presents the radiation pattern of the arrays optimized by the proposed method and by the ordinary method. In the ordinary method, full wave simulation is performed to calculate the array radiation pattern in every iteration. From Figure 8, it can be seen that the proposed method results in the same optimized radiation pattern as the ordinary method. Figure 9 shows the locations of active elements. The percentage of active elements is 89%. Figure 10 presents the variation of PSLL as genetic optimization goes on. From Figure 9 and Figure 10, one can observe that both the number of elements and PSLL are reduced by using proposed method. Table 2 presents performance comparison between the proposed

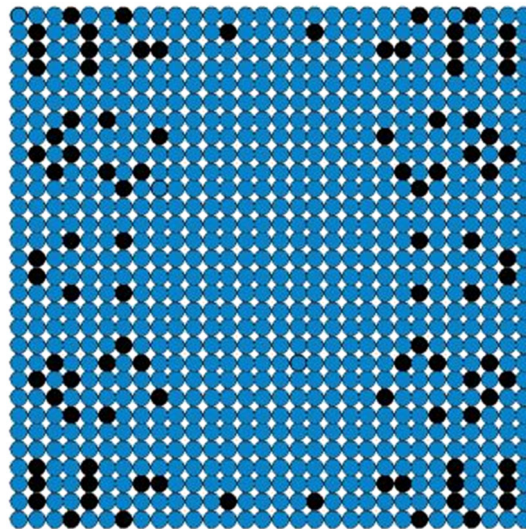


**FIGURE 6** Array geometry revealing the active and dummy element. The active elements are in gray color and the dummy elements are in black color

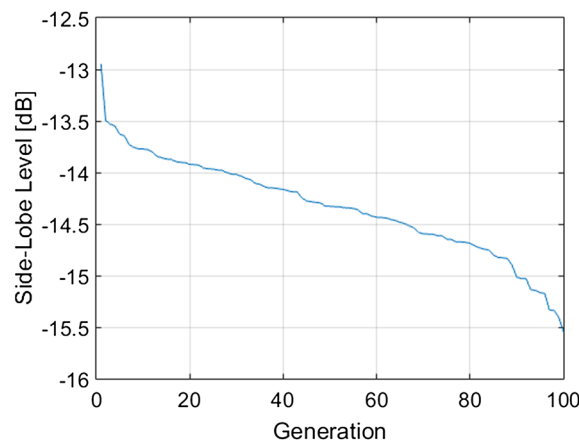


**FIGURE 7** PSLL (dB) of the dipole array versus stages of evolution

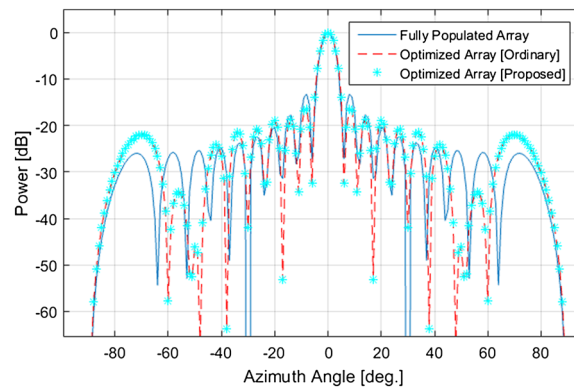


**FIGURE 8** View of the array radiation pattern at  $\theta = 0^\circ$ ,  $\phi$  varies from  $-90^\circ$  to  $90^\circ$

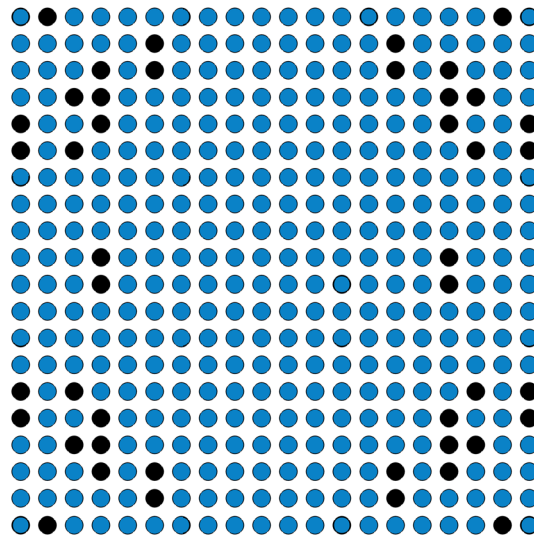


**FIGURE 9** Array geometry revealing the active and dummy elements. The active elements are in gray color and the dummy elements are in black color

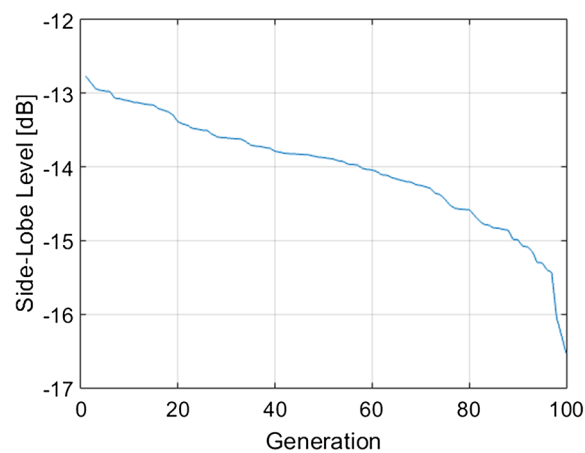


**FIGURE 10** Peak side lobe level (PSLL; dB) of the patch antenna array versus stages of evolution



**TABLE 2** Optimization results summary for the patch antenna

Optimization time Condition	Ordinary method 8.25 h		Proposed method 3.39 h	
	Full array	Optimized array	Full array	Optimized array
Main-lobe	41.91 dB	40.93 dB	41.91 dB	40.93 dB
Peak side-lobe level (normalized)	−13.25 dB	−16.54 dB	−13.25 dB	−16.54 dB
Active elements	100% (400)	89% (356)	100% (400)	89% (356)
Dummy elements	0	44	0	44

method and ordinary method. It can be seen that the proposed significantly reduced the optimization time without performance loss.

## 4 | CONCLUSIONS

This paper presented an efficient method for optimizing sparse antenna arrays by using Green's function and GA. The radiation pattern of the array has been efficiently calculated by using the NGF. The status of every array element is represented by using binary coding, and the array is thinned by genetic optimization. A dipole array has been used to validate the proposed method, and a patch antenna array has been optimized to demonstrate the advantage of the proposed method. It has been shown that the proposed method significantly reduced the optimization time.

## ACKNOWLEDGEMENTS

This work was partially supported by the National Natural Science Foundation of China (Grant/Award Number: 61701087) and the Sichuan Science and Technology Program (Grant/Award Number: 18GJHZ).

## ORCID

Huapeng Zhao  <https://orcid.org/0000-0002-2036-5344>

## REFERENCES

1. Liu Y, Liu QH, Nie Z. Reducing the number of elements in multiple-pattern linear arrays by the extended matrix pencil methods. *IEEE Trans Antennas Propag.* 2014;62(2):652-660.
2. Gao S, Zhao H, Deng H, Wang B, Zhao W. Estimating interference to airborne patch antennas with limited information. *IEEE Trans Electromagn Compat.* 2016;58(2):631-634.
3. Du Q, Ren H, Png CE, Wang H-T. Extremely sharp transmission peak in optically thin aluminum film with hexagonal nanohole arrays. *J Opt.* 2018;20(10):105002.
4. Daniel P, Marco DM, Mario L, Fulvio S. On the comparison and evaluation of sparse array synthesis methods. *Int Appl Comput Electromagn Soc Symp.* 2017;1-2.
5. Fasenfest BJ, Capolino F, Wilton DR. Preconditioned GIFFT: a fast MoM solver for large arrays of printed antennas. *Int Appl Computat Electromagn Soc Symp.* 2006;21(2):276-283.
6. Bray MG, Werner DH, Boehringer DW, Machuga DW. Optimization of thinned aperiodic linear phased arrays using genetic algorithms to reduce grating lobes during scanning. *IEEE Trans Antennas Propag.* 2002;50(12):1732-1782.
7. Brahma P, Nandi P, Senapati A, Roy JS. Reduction of side-lobe level of thinned phased array antenna using genetic algorithm. *Int J Comput Appl.* 2015;112:13-15.
8. Gao S, Zhao H, Zhao W, Liu E. Equivalent model built with limited information: predicting installed performance of slotted waveguide antennas. *IEEE Antennas Propag Mag.* 2018;52(5):52-61.
9. Gao S-P, Wang B, Zhao H, Zhao W-J, Png CE. Installed radiation pattern of patch antennas: prediction based on a novel equivalent model. *IEEE Antennas Propag Mag.* 2015;57(3):81-94.
10. Orfanidis SJ. "Electromagnetic waves and antennas" Rutgers University. 2016;731-729.



11. Markarov SN, Kulkarni SD, Marut AG. Method of moments solution for a printed patch/slot antenna on a thin film dielectric substrate using the volume integral equation. *IEEE Trans Antenna Propag.* 2016;54(4):1174-1184.
12. Jakobus U, Bingle M, Burger W, Ludick D, Schoeman M, Van Tonder J. "Method of moments accelerations and extensions in FEKO," International Conference on Electromagnetics in Advanced Applications. 2011;62-65.
13. Nandi P. "Optimization of side-lobe level of thinned phased array antenna using genetic algorithm and particle swarm optimization," IEEE International WIE Conference on Electrical and Computer Engineering, pp. 27-30, 2015.
14. Sappal AS. Design of rectangular microstrip patch antenna using particle swarm optimization. *International Journal of Advanced Research in Computer and Communication Engineering.* 2013;2:7.
15. Ahamed M, Bhowmik K, Suman A. Analysis and design of rectangular microstrip patch antenna on different resonant frequencies for pervasive wireless communication. *Int J Sci Technol Res.* 2012;5:1.
16. Nourinia J., "Side-lobe level optimization in phased array antennas using genetic algorithm," Eighth IEEE International Symposium on Spread Spectrum Technology Application Australia. 2004;389-393.

**How to cite this article:** Raji MF, Zhao H, Monday HN. Fast optimization of sparse antenna array using numerical Green's function and genetic algorithm. *Int J Numer Model.* 2020;33:e2544. <https://doi.org/10.1002/jnm.2544>